Journal of Integral Sciences
[An International Open Access Journal]
Available at www.jisciences.com ISSN: 2581-5679

STRUCTURE-PERFORMANCE RELATIONSHIPS IN COUPLING REAGENTS: A REVIEW OF DFT- AND QSPR-GUIDED DESIGN OF AZO CHROMOGENS FOR DRUG DETERMINATION

WALAA MOHAMMED NAJEM

College of Medical Laboratory Techniques, Imam Ja'afar Al-Sadiq University, Najaf, Iraq

Received: 14-06-2026 Revised: 09-07-2026 Accepted: 22-08-2026

ABSTRACT

Diazotization followed by azo coupling is still one of the most heavily used derivatization routes in pharmaceutical UV-visible spectrophotometry, and yet the selection of the coupling reagent is very often made by trial and error, or simply by copying whatever the previous paper in the same journal happened to use. This review asks a narrower question than the usual survey of applications: what structural features of a coupler actually control the analytical figures of merit, and how far can density functional theory (DFT) and quantitative structure-property relationships (QSPR) replace that guesswork with prediction? We revisit the coupling step as an electrophilic aromatic substitution whose rate, regiochemistry and pH window are set by the ionization state of the coupler and by the electrophilicity of the arenediazonium ion generated from the drug. We then connect those variables to the quantities an analyst actually cares about: absorption maximum, molar absorptivity and colour stability. Conceptual-DFT indices, in particular the electrophilicity index, the nucleophilicity index and condensed Fukui functions, are shown to rationalize reagent behaviour that is otherwise reported as an empirical observation. Time-dependent DFT reproduces azo absorption maxima to within roughly 6-12 nm when the functional and the solvation model are chosen with care, while recent QSPR and machine-learning models predict λ_{max} across hundreds of azo dyes with external coefficients of determination approaching 0.9. A structure-performance map of the common couplers is assembled, recurring errors in present computational practice are identified, and a minimum reporting set is proposed.

Keywords: *Azo coupling; coupling reagent; density functional theory; QSPR; spectrophotometry; drug determination; azo-hydrazone tautomerism; green analytical chemistry.*

***Corresponding Author**
Walaa Mohammed Najem

DOI: https://doi.org/10.37022/jis.v9i2.150

Produced and Published by
South Asian Academic Publications

1. INTRODUCTION

Visible spectrophotometry has not gone away. Despite four decades of chromatographic dominance in pharmaceutical quality control, colour-forming assays are still written, validated and published in large numbers, mostly because they need almost no instrumentation and can be run where a liquid chromatograph is neither affordable nor maintainable [1-9]. Among these assays, the diazotization-coupling family occupies a peculiar position. It is chemically old, it is extremely well documented, and it has been applied to an enormous span of analytes, from sulfonamides and cephalosporins through to kinase inhibitors developed only in the last few years [10, 11].

What has changed much less is how the coupling reagent gets chosen. Reading through the recent literature one finds the same short list of couplers, 1-naphthol, 2-naphthol, resorcinol, chromotropic acid, 8-hydroxyquinoline, phloroglucinol, recycled from paper to paper, and the justification given is usually retrospective: the reagent gave a strong colour, therefore it was suitable [12-14]. Screening several couplers and reporting the best absorbance is legitimate, but expensive, it consumes reagents that green analytical chemistry would rather we did not consume [15], and it produces no transferable knowledge. The next analyte starts the screen again from zero, and in effect each laboratory rediscovers the same handful of empirical facts.

There is now a reasonable case that this can be done differently. Quantum-chemical treatments of analytical azo coupling appeared as early as the mid-2000s [16], conceptual DFT has matured into a stable set of

reactivity indices [17], and structure-property modelling of dye colour has moved from small regression models to machine learning trained on several hundred azo compounds [7, 18]. What is missing is the connecting tissue: an account of which computed quantity maps onto which analytical figure of merit, and how reliable that mapping actually is. That is what the present review attempts.

2. THE COUPLING STEP, REVISITED FROM AN ANALYTICAL POINT OF VIEW

2.1 The electrophile derived from the drug

In the overwhelming majority of pharmaceutical applications the drug supplies the amine. A primary aromatic amino group, either present in the molecule as supplied or liberated by acid or alkaline hydrolysis, is treated with sodium nitrite in a cold mineral-acid medium to give the arenediazonium ion. The electrophilicity of that ion is not a constant; it responds strongly to the substituents carried by the drug, and the same substituents govern how fast the ion decomposes before it has a chance to couple [19]. This is the first practical consequence for method development. Electron-withdrawing groups raise diazonium reactivity and, at the same time, tend to improve thermal stability, whereas strongly electron-donating substituents give a sluggish, short-lived electrophile that demands tight temperature control. Systematic kinetic work on para-substituted benzenediazonium cations places the reaction squarely within the Mayr electrophilicity-nucleophilicity framework and yields substituent relations of the Hammett type [20, 21]. For a series of 3-aminothiophene couplings, for instance, the nucleophile parameters $N = 9.37$ and $s_N = 1.18$ were obtained together with the relation $N = 6.72 - 2.01\sigma^{+}$, with carbon attack rate-determining [21].

Drugs that carry no diazotizable amine are handled either by pre-derivatization, most commonly reduction of a nitro group or hydrolysis of an amide, or by inverting the roles so that the drug acts as the coupler and an auxiliary aromatic amine supplies the diazonium ion. Paracetamol is the textbook case of the first strategy [12, 22], methyldopa and phenylephrine of the second [23, 24]. The distinction matters more than it may seem, because in the inverted mode the analyte's own electronic structure determines the nucleophilicity, and the design problem shifts from choosing a coupler to choosing a diazotized reagent.

2.2 What makes a coupler a good coupler

Azo coupling is an electrophilic aromatic substitution, and the classical kinetic analysis established that the reactive species is the ionized form of the coupler: the phenolate for phenols and naphthols, the free base for aromatic amines [1, 2]. Later kinetic work on pyrazolinone couplers put numbers on this, locating the relevant pK_a at 5.07 at 293 K and establishing a Hammett correlation in which electron-withdrawing groups on the diazonium partner accelerate attack [25]. Everything else follows from that. A coupler is effective when it can be deprotonated, or kept unprotonated, under conditions where the diazonium ion has not yet decomposed, and when the resulting anion carries a high electron density at a sterically accessible ring position. Naphthols satisfy this better than simple phenols, which is why 1-naphthol and 2-naphthol dominate the applied literature. Polyhydroxy couplers such as resorcinol and phloroglucinol go further, since successive hydroxyls raise the nucleophilicity of the ring and lower the pH at which the reactive anion becomes available [13, 22].

Regiochemistry is the second consideration, and it is not fixed. Skrabal and Zollinger showed that the ortho/para ratio in aminohydroxynaphthalene couplers is set by which ionized form predominates at a given pH, so that pH controls not only the rate but the identity of the product [26, 27]. Bulky substituents adjacent to the coupling site can shift the rate-determining step from attack of the diazonium ion to the subsequent proton loss, which changes how the observed rate responds to buffer composition [28]. Analysts rarely check for this, and it is a plausible reason why some published procedures show an inexplicably narrow optimum in buffer concentration.

Side reactions deserve more attention than they normally get. Amine couplers can react at nitrogen to give triazenes, which subsequently rearrange to the C-azo product, so an apparently slow colour development may in fact be a two-stage process [29]. Triazenes are also considerably more thermally stable than the parent diazonium salts, a point established quantitatively in a process-chemistry context but with obvious implications for reagent blank behaviour [30]. Heteroaromatic diazonium ions follow their own reactivity ordering [31], and medium effects, including ion pairing with anionic surfactants, can accelerate coupling appreciably [32]. Table 1 sets out the couplers that recur in the pharmaceutical literature together with the species that actually reacts in each case, and Figure 1 collects the three mechanistic strands discussed above. The standard monographs remain the best entry point to this literature [33, 34].

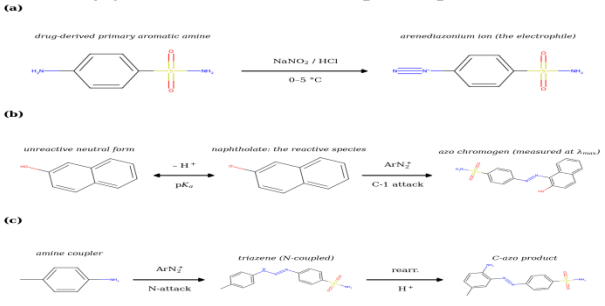

Figure 01: Mechanistic anatomy of the analytical azo-coupling reaction: (a) diazotization of the drug-derived primary aromatic amine; (b) pH-dependent speciation of a representative naphthol coupler and C-1 attack by the arenediazonium ion; (c) the competing N-coupling pathway that yields a triazene and its rearrangement to the C-azo product.

Table 01: Coupling reagents recurring in the pharmaceutical azo assays surveyed here, with their chemical class, the species that actually reacts under assay conditions, the role each plays in the determination, and a representative analyte.

Coupling reagent	Chemical class	Reactive species	Role	Representative analyte	Ref.
1-Naphthol	Naphthol	Naphtholate anion	Coupler	Metoclopramide; paracetamol; futibatinib	[11, 22, 36].
2-Naphthol (β-naphthol)	Naphthol	Naphtholate anion	Coupler	Sulfanilamide; cefixime; paracetamol	[12, 37, 39].
Resorcinol	1,3-Dihydroxybenzene	Mono-phenolate	Coupler	Paracetamol	[22].
Phloroglucinol	1,3,5-Trihydroxybenzene	Phenolate	Coupler	Bromhexine hydrochloride	[13].
Chromotropic acid	Dihydroxynaphthalene-disulfonic acid	Di-anion	Coupler	Cefixime; sildenafil citrate	[14,[56].
8-Hydroxyquinoline	Quinolinol	Quinolinolate	Coupler	Paracetamol	[12]
p-Dimethylamino-benzaldehyde	Tertiary aromatic amine	Free base	Coupler	Ceftriaxone, ceftazidime, cefixime, cefotaxime, cefuroxime	[53]
Alanine; tyrosine	α-Amino acids	Free amine / phenolate	Coupler	Paracetamol	[52]
Anthranilic acid; 2-aminopyrimidine	Aromatic / heteroaromatic amine	Arenediazonium ion	Diazotized partner	Methyldopa	[23]
Sulfanilic acid	Aromatic sulfonic amine	Arenediazonium ion	Diazotized partner	Minoxidil	[38]
Sulfacetamide sodium	Sulfonamide	Arenediazonium ion	Diazotized partner	Phenylephrine hydrochloride	[24]
1-Amino-4-nitro-naphthalene	Nitro-naphthylamine	Arenediazonium ion	Diazotized partner	Doxycycline	[51]
4-Aminoacetophenone	Aromatic ketone amine	Arenediazonium ion	Diazotized partner	Genistein	[54]
4-(2-Thiazolylazo)-resorcinol and analogues	Preformed azo ligand	Chelating anion	Ternary chromogen	Vanadium(V); cobalt(II) (sensitivity benchmarks)	[40],[41]

3. WHERE THE ANALYTICAL FIGURES OF MERIT COME FROM

3.1 Absorption maximum and molar absorptivity

The two numbers that decide whether a method is worth publishing are λ_{max}, because it determines how far the measurement sits from formulation excipient interference, and the molar absorptivity, because it fixes the detection limit. Both are properties of the extended donor-acceptor system created when the azo bridge links the two rings. Push-pull architectures, in which an electron donor on one ring faces an acceptor on the other, produce intramolecular charge-transfer bands that are red-shifted and intense [35]. This is the same design logic used in disperse dyes and in nonlinear optical materials, and it transfers directly to analytical reagents.

Numbers from the applied literature bear this out, although with a good deal of scatter. Coupling metoclopramide with 1-naphthol gives λ_{max} at 550 nm with ε close to 3.5×10^4 L mol^{-1} cm^{-1} [36], while the sulfanilamide-β-naphthol product absorbs at 489 nm with ε near 2.9×10^4 [37]. At the other end, the minoxidil-sulfanilic acid system absorbs at 400 nm

with ε of only about 4.6 × 10^3, and the reported detection limit is nonetheless very low, which raises questions about how that limit was estimated [38]. Chromotropic acid, being both strongly activating and water-soluble, tends to give products further into the visible: cefixime coupled with chromotropic acid absorbs at 514 nm [14] against 412 nm for the same drug coupled with β-naphthol [39]. Sensitivity can be pushed much further by moving the coloured product into a small volume of surfactant-rich or organic phase; cloud-point extraction of azo complexes has delivered ε values above 10^5 and Sandell sensitivities below 1 ng cm^{-2} [40, 41], and dispersive liquid-liquid microextraction has been coupled to azo-dye formation for tetracycline in real samples [42].

3.2 Tautomerism and solvatochromism as hidden variables

Hydroxy-azo dyes exist as an equilibrium between the azo and the hydrazone form, and the two tautomers do not have the same colour. This is a well-studied problem in dye chemistry [43] and is summarized in Figure 2, but it is rarely acknowledged in analytical papers, where a single λ_{max} is quoted as if it were a fixed constant of the product. It is not. Solvent composition alone can move the position of the equilibrium in naphthol-derived chromogens developed specifically as reagents for drug assay [44],[45], and spectral deconvolution of common azo dyes shows some to be predominantly hydrazone and others predominantly azo in the same solvent [46]. Ring substituents shift both the tautomeric position and the acid-base behaviour in a correlated way [47]. In one arylazo system a Hammett correlation with r^2 = 0.983 and ρ = 1.07 was obtained alongside a Kamlet-Taft treatment across eight solvents, with multiple correlation coefficients between 0.810 and 0.993 [48].

The practical corollary is uncomfortable. If a validated procedure specifies an ethanol-water measurement medium and a subsequent laboratory substitutes methanol, the tautomeric balance may shift enough to move λ_{max} by several nanometres and to change ε, and the transferred method will quietly lose sensitivity without any obvious failure. Acidity constants of the chromogen, best obtained by multiwavelength treatment of pH-dependent spectra rather than by single-wavelength titration [49], should therefore be regarded as part of the method description and not as an optional characterization exercise.

Colour stability is the third neglected variable. Azo dyes in aqueous solution degrade at rates that are strongly temperature-dependent; for tropaeolin OO the pseudo-first-order constant rises from 0.036 h^{-1} at 20 °C to 0.325 h^{-1} at 50 °C, and calcon behaves similarly on a smaller scale [50]. Reducing agents present in the sample matrix, ascorbic acid being the obvious example, accelerate this. A stability window quoted as "the colour was stable for 60 min" without stating the temperature is close to meaningless.

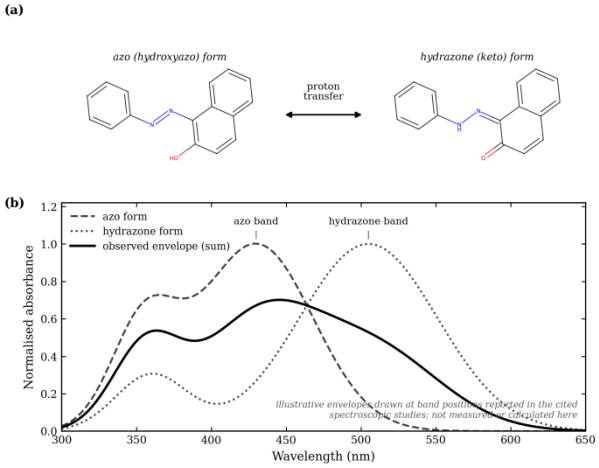

Figure 02: Azo-hydrazone tautomeric equilibrium in a naphthol-derived chromogen and its spectral consequence: (a) the two tautomeric forms of 1-phenylazo-2-naphthol; (b) illustrative absorption envelopes drawn at the band positions reported in the cited spectroscopic studies, showing how the observed spectrum is a weighted sum of the two forms rather than a single fixed band.

4. PREVIOUS STUDIES: WHAT THE PUBLISHED CORPUS ACTUALLY SHOWS

A survey of diazotization-coupling assays published over roughly the last fifteen years gives a fairly consistent picture, and also exposes some persistent weaknesses. The most recent dedicated review, covering the 2010-2023 window, organizes the field by analyte class, aromatic amines, nitro compounds, phenols, hydrazine derivatives and aliphatic amines, and attributes the sensitivity of the approach to the intense visible absorption of the azo product [10]. That classification is useful but it is analyte-centred; it does not tell a method developer which reagent to pick.

Table 2 compiles representative assays from this body of work, and Figure 5 plots the same data as absorption maximum against detection limit. Looking instead across couplers, several regularities emerge. Naphthols give the longest-wavelength products and the highest molar absorptivities among the simple couplers, with reported ranges of 0.4-18 μg mL^{-1} for metoclopramide [36] and 1-12 μg mL^{-1} for sulfanilamide [37]. Resorcinol and 1-naphthol applied to the same analyte, hydrolysed paracetamol, gave 480 and 510 nm respectively with comparable linear ranges, which is a rare and useful head-to-head comparison [22]. Phloroglucinol, used for bromhexine in an alkaline medium, gave a short-wavelength product at 405 nm but a very low detection limit of 0.087 μg mL^{-1} [13]. 8-Hydroxyquinoline and 2-naphthol

applied to paracetamol produced 470 and 490 nm products with ε around 1.9 × 10^4 for the former [12]. Nitro-substituted naphthylamines have also served as the diazotized partner, as in a doxycycline assay reading at 466 nm with a detection limit of 0.297 μg mL^{-1} [51]. Unconventional couplers appear from time to time, including amino acids such as alanine and tyrosine, which gave workable but distinctly less sensitive assays with detection limits of 1.27 and 1.74 μg mL^{-1} [52], and p-dimethylaminobenzaldehyde applied across five cephalosporins with detection limits between 1.75 and 6.15 μg mL^{-1} [53].

Several trends run through the corpus. First, the assays are almost always applied to bulk drug and to simple solid dosage forms; biological matrices are rare. Second, the sensitivity ceiling of the direct batch procedure sits around 10^4 to 10^5 L mol^{-1} cm^{-1}, and getting beyond it requires either preconcentration [54],[42] or a metal-containing ternary system [55],[56]. Third, and most relevant here, computational support is nearly absent. Where it appears it is usually a single geometry optimization and a frontier-orbital picture presented after the fact [11]. Fourth, stoichiometry is almost always claimed from a Job plot, often without acknowledging the well-documented assumptions on which the method of continuous variations rests [57].

Table 02: Representative diazotization-coupling spectrophotometric assays of pharmaceuticals, listing the coupling system, analyte, absorption maximum, molar absorptivity, linear range and detection limit exactly as reported by the original authors.

Coupling system (coupler / diazotized partner)	Analyte	λmax (nm)	ε (L mol^{-1} cm^{-1})	Linear range (μg mL^{-1})	LOD (μg mL^{-1})	Ref.
1-Naphthol / metoclopramide	Metoclopramide HCl	550	3.50 × 10^4	0.4–18	0.545	[36]
1-Naphthol / paracetamol	Paracetamol	510	n.r.	2.5–20	n.r.	[22]
Resorcinol / paracetamol	Paracetamol	480	n.r.	3–15	n.r.	[22]
2-Naphthol / sulfanilamide	Sulfanilamide	489	2.88 × 10^4	1–12	0.247	[37]
2-Naphthol / cefixime	Cefixime	412	n.r.	1–20	0.109	[39]
2-Naphthol / paracetamol	Paracetamol	490	n.r.	2–10	n.r.	[12]
8-Hydroxyquinoline / paracetamol	Paracetamol	470	1.9 × 10^4	2–10	n.r.	[12]
Chromotropic acid / cefixime	Cefixime	514	n.r.	0.5–20	0.322	[14]
Phloroglucinol / bromhexine	Bromhexine HCl	405	n.r.	0.25–15	0.087	[13]
Phenylephrine / sulfacetamide	Phenylephrine HCl	425	n.r.	2–24	0.278	[24]
Doxycycline / 1-amino-4-nitronaphthalene	Doxycycline	466	n.r.	0.5–20	0.297	[51]
Minoxidil / sulfanilic acid	Minoxidil	400	4.62 × 10^3	5–40	0.012	[38]
Methyldopa / anthranilic acid	Methyldopa	455	n.r.	6.25–62.5*	n.r.	[23]
Methyldopa / 2-aminopyrimidine	Methyldopa	450	n.r.	6.25–62.5*	n.r.	[23]
Alanine / paracetamol	Paracetamol	n.r.	n.r.	2–30	1.266	[52]
Tyrosine / paracetamol	Paracetamol	n.r.	n.r.	2–30	1.737	[52]
p-Dimethylaminobenzaldehyde / five cephalosporins	Ceftriaxone, ceftazidime, cefixime, cefotaxime, cefuroxime	400–430	n.r.	5–60	1.751–6.152	[53]
Genistein / 4-aminoacetophenone, cloud-point extraction	Genistein	437	n.r.	0.25–2.75	n.r.	[54]
Genistein / 4-aminoacetophenone, flow injection	Genistein	437	n.r.	10–100	n.r.	[54]

Coupling system (coupler / diazotized partner)	Analyte	λmax (nm)	ε (L mol⁻¹ cm⁻¹)	Linear range (μg mL⁻¹)	LOD (μg mL⁻¹)	Ref.
4-(2-Thiazolylazo)resorcinol / V(V)–H_2O_2, cloud-point extraction†	Vanadium(V)	569	7.4×10^4	0.006–0.510	0.0017	[40]
Hydrophobic thiazolylazoresorcinol / Co(II), cloud-point extraction†	Cobalt(II)	553	2.63×10^5	0.0054–0.189	0.00164	[41]

n.r. = not reported in the source consulted. * Linear range quoted by the original authors in mg L^{-1}. † Metal-ion systems included as sensitivity benchmarks for preconcentrated azo chromogens, not as drug assays.

5. DFT AS A DESIGN TOOL FOR COUPLING REAGENTS

5.1 Global reactivity indices and the pairing rule

Conceptual DFT provides a compact vocabulary for reactivity: chemical potential and its negative, electronegativity; chemical hardness and softness; and the electrophilicity index $\omega = \mu^2/2\eta$ introduced by Parr and co-workers [3],[17]. The complementary nucleophilicity index N was later put on an empirical footing by Domingo and Pérez [4]. Together they support a simple pairing rule that is directly applicable to analytical azo coupling: a fast, quantitative reaction requires a strongly electrophilic diazonium partner and a strongly nucleophilic coupler, and the larger the difference in these indices, the more polar and the more rapid the process. Working thresholds are available, with ω above 1.5 eV describing a strong electrophile and values below 0.8 eV a marginal one, and correlations between ω and computed activation energies as high as $R^2 = 0.92$ have been reported for well-behaved reaction series [58].

Table 3 lists these descriptors with their definitions and their analytical reading. Applied to azo chemistry, these indices behave sensibly. Reactive Orange 16 is classed as a strong electrophile with ω above 1.5 eV and a moderate nucleophile once solvation is included [59], and across a series of substituted azobenzene disperse dyes the aldehyde derivative showed both the highest electrophilicity index, 4.6441 eV, and the largest dipole moment, 4.9366 D [6]. Complexation shifts the picture dramatically: an azo dye ligand with a HOMO-LUMO gap of 3.42 eV yielded chelates with gaps between 1.01 and 2.56 eV depending on the metal [60], and a comparable ordering was found for nitroxoline azo complexes [61]. For the analyst, the useful implication is that a ternary system does not merely add colour, it produces a genuinely different, softer and more polarizable chromophore.

5.2 Local descriptors and regioselectivity

Global indices say whether a pair will react; they cannot say where. That is the role of the Fukui function, defined by Parr and Yang as the response of the electron density to a change in electron number [62], and of its condensed-to-atom form obtained from population analysis [63]. For a coupler, the relevant quantity is f^-, the index for electrophilic attack; the ring atom with the largest f^- in the deprotonated species should be the coupling site. Molecular electrostatic potential maps give a complementary and more visual reading of the same information, and natural bond orbital analysis quantifies the donor-acceptor stabilization that follows [64],[65]. An early quantum-chemical treatment of analytical azo coupling specifically concluded that orbital control, together with aqueous solvation, directs the diazonium ion to the 4-position of 1-aminonaphthalene [16], which is exactly the kind of prediction a method developer could act on.

Figure 3 makes this concrete for the coupler that appears most often in these assays. Optimized at B3LYP/6-31G(d) with a continuum water model, 2-naphthol has its highest occupied orbital at −5.67 eV; deprotonation lifts it to −3.96 eV and narrows the frontier gap from 4.67 to 3.76 eV, while the Koopmans electrophilicity index drops from roughly 2.38 to 1.15 eV. In both species the largest carbon f^- lies at C-1, which is where β-naphthol is in fact observed to couple, though in the anion the oxygen itself carries the largest index of all, a reminder that the softest site is not automatically the one that gives a stable product.

In practice these calculations are cheap. A geometry optimization at B3LYP/6-31G(d,p) or 6-311G(d,p) with an implicit solvent model, followed by single-point calculations on the cation and anion, delivers the whole descriptor set in a few processor-hours for molecules of this size. The barrier is not cost. It is that the deprotonated form, the species that actually reacts, is frequently not the one calculated.

5.3 TD-DFT and the prediction of colour

Predicting λ_{max} is where TD-DFT earns its place, and the accuracy achievable is now reasonably well characterized for azo systems specifically. For twenty-two azoalkane derivatives, PCM-TD-PBE0 reproduced the n→π* wavelength with a mean absolute error of 5.8 nm, or 0.056 eV, with a worst case of 21 nm [5]. A benchmark across eight functionals on azo sulfonamide fluorochromes found PBE-based functionals deviating by only 0.06-0.12 eV, B3LYP and O3LYP overestimating by 0.17-0.26 eV, and range-separated functionals underestimating by anything from 0.15 to 0.52 eV [66]. More recent applied studies report deviations of 12 nm or less for azobenzene disperse dyes at B3LYP/6-31G(d,p) [6] and good reproduction of experimental maxima over the 360-440 nm range for barbituric azo dyes [67]. Azobenzene-

based photochromic systems modelled with CAM-B3LYP gave maxima at 430 and 440 nm with gaps of 2.42-2.54 eV [68], and TD-DFT with PCM across eight solvents has been used to track solvatochromic shifts in monoazo disperse dyes [69].

Three caveats deserve emphasis. Gas-phase calculations are of little use for reagents that work in buffered aqueous media, so an implicit solvent model is a minimum requirement and explicit water molecules are sometimes needed where hydrogen bonding is cooperative [43]. Charge-transfer states are poorly described by conventional hybrids, which is precisely the situation in a strong push-pull azo dye, so functional choice cannot be treated as a formality. And the tautomer question returns here in an acute form: computing only the azo form of a hydroxy-azo chromogen and comparing the result with an experimental spectrum that contains both tautomers is a category error, however good the agreement happens to look.

Table 03: Conceptual-DFT descriptors most frequently reported for azo chromogens, with their working definition and the reading a reagent designer should take from each.

Descriptor	Working definition	What it tells the reagent designer	Key Ref.
Ionization potential, I	$I \approx -E(HOMO)$ (Koopmans)	Ease of removing electron density from the coupler; a low I marks a strong donor	[17]
Electron affinity, A	$A \approx -E(LUMO)$	Capacity of the diazonium partner to accept electron density	[17]
Electronegativity, χ	$\chi = (I + A)/2$	Direction of charge flow when the two partners meet	[17]
Chemical potential, μ	$\mu = -\chi$	Escaping tendency of the electron cloud	[17]
Chemical hardness, η	$\eta = (I - A)/2$	Resistance to charge transfer; soft couplers react faster with soft electrophiles	[17]
Chemical softness, S	$S = 1/(2\eta)$	Complement of hardness; tracks polarizability of the chromophore	[17]
Electrophilicity index, ω	$\omega = \mu^2/(2\eta)$	Strength of the diazonium electrophile; ω > 1.5 eV marks a strong electrophile	[3],[58]
Nucleophilicity index, N	N = E(HOMO)nu − E(HOMO)TCE	Donor strength of the coupler on an empirical, transferable scale	[4]
Fukui function, f(r)	$f(r) = [\partial\rho(r)/\partial N]v$	Site-resolved response of the electron density to electron gain or loss	[62]
Condensed Fukui index, f^-	$f^-k = qk(N-1) - qk(N)$	Ranks ring positions for electrophilic attack; the largest f^- is the expected coupling site	[63]
Molecular electrostatic potential (MEP)	V(r) from the total charge density	Visual map of the electron-rich region the diazonium ion will approach	[65]
NBO stabilization energy, E(2)	Second-order donor→acceptor perturbation energy	Quantifies the charge transfer that generates colour in the azo product	[64]
HOMO–LUMO gap	$\Delta E = E(LUMO) - E(HOMO)$	First-order guide to λmax and to the softness of the chromophore	[60]

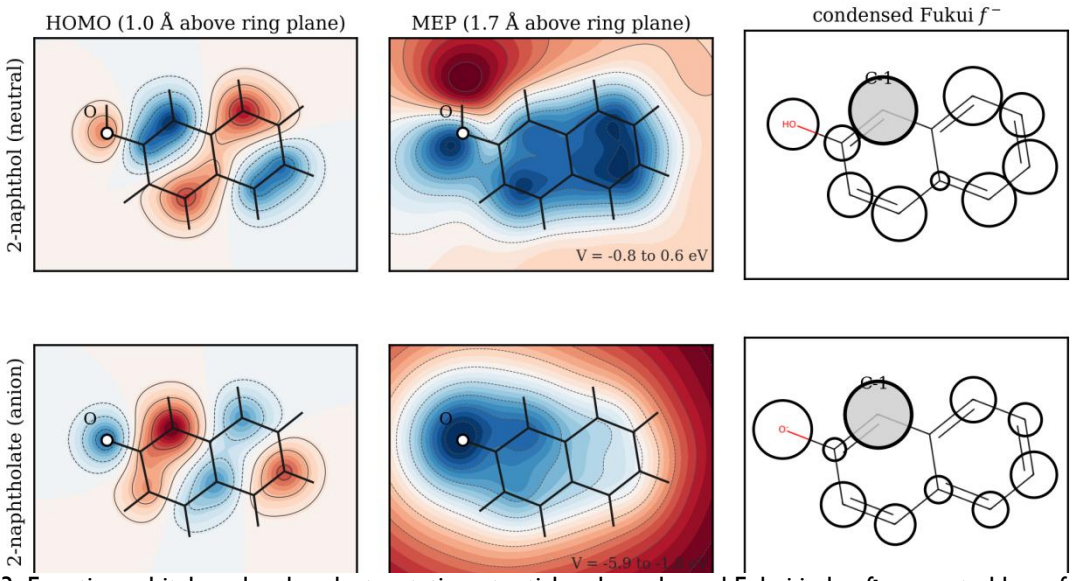

Figure 03: Frontier orbital, molecular electrostatic potential and condensed Fukui index f^- computed here for 2-naphthol and its conjugate base at B3LYP/6-31G(d) with a continuum water model, showing how deprotonation raises the donor orbital and concentrates nucleophilic character at C-1. The orbital and potential panels are sections taken 1.0 and 1.7 Å above the mean ring plane; in the right-hand panels the circle areas are proportional to f^-, with hydrogen contributions folded onto the attached heavy atom.

6. QSPR AND MACHINE LEARNING: FROM ONE MOLECULE TO A REAGENT LIBRARY

6.1 Models for the absorption maximum

DFT treats one molecule at a time. QSPR treats a population, and for screening a candidate reagent library that is the more efficient posture. Modelling of azo dye colour has a respectable history: an early descriptor-based study addressed azobenzene λ_{max} directly [70], and ant colony optimization was introduced as a descriptor-selection engine for the same endpoint and then extended to anthraquinone dyes [71],[72]. Table 4 summarizes what these models achieve. The field has since moved on considerably. Deep neural networks trained on structural input rather than hand-selected descriptors now predict λ_{max} across broad chemical space [73], and support-vector models built on fragment-count descriptors for 798 azo compounds reached an external R^2 of 0.905 with a cross-validated RMSE of 21.6 nm [7].

The most directly relevant recent study couples TD-DFT descriptors with machine learning. Working with 197 azo dyes split into 160 training and 37 test compounds, and with descriptors computed at B3LYP/6-31G(d,p) under SMD solvation, Gaussian process regression gave leave-one-out R^2 of 0.837 with an RMSE of 18.9 nm, falling to R^2 = 0.736 and RMSE = 31.5 nm on the independent test set; SHAP analysis was then used to interpret the model, and 14,376 candidate structures were screened virtually [18]. That workflow is essentially the template this review would recommend for coupler design, although it has not yet been applied to analytical reagents.

A word of caution about the numbers. An RMSE of 20-30 nm sounds modest against a visible range of some 400 nm, but for anyone trying to place a product band clear of a formulation excipient it is a large uncertainty. These models rank candidates well; they do not substitute for measurement.

6.2 Descriptors, endpoints and the endpoints that are missing

Descriptor generation is no longer a bottleneck, with open-source tools such as PaDEL and Mordred producing hundreds to thousands of two- and three-dimensional descriptors from a structure file [74],[75]. The bottleneck is the endpoint. Almost all published dye QSPR work targets λ_{max}, for the simple reason that λ_{max} is what dye databases record. Molar absorptivity, which matters more for an analytical reagent, has been addressed far less often, and the one systematic attempt across dye classes frames the question as an open one [76]. Colour stability, selectivity against excipients and tolerance to matrix reductants have, as far as we are aware, never been modelled at all. A recent review of QSPR and machine learning in molecular photonics confirms this imbalance across the wider field [77].

There is also a useful precedent from analytical chemistry itself that is rarely cited in the dye literature: quantitative structure-retention relationships have been used for decades to predict a measured instrumental response from structure, and the methodological lessons learned there about descriptor selection and model transferability apply almost unchanged [78].

6.3 Validation is not optional

If computational reagent selection is to be taken seriously by analysts, the models behind it must meet the same standards as the analytical methods themselves. Internal cross-validation is insufficient on its own; external test-set validation is required, and y-randomization should be reported [79],[80]. Several external-validation metrics beyond Q^2 exist and behave differently, so more than one should be quoted [81]. Above all, the applicability domain has to be defined, since a model trained on textile dyes will happily extrapolate to a sulfonamide-derived chromogen and return a confident and meaningless number; leverage-based and distance-based approaches are both available and have been compared systematically [82]. The five OECD validation principles, whose origin and rationale have recently been reviewed, provide the accepted framework [83].

Table 04: Published QSPR and machine-learning models for the absorption maximum of azo dyes, showing the chromophore set, descriptor space, algorithm, and the internal and external validation statistics as reported.

Study	Chromophore set (n)	Descriptor space	Algorithm	Internal validation	External validation
[70]	Azobenzene dyes	Calculated molecular descriptors	QSPR (linear and non-linear)	n.r. in the record consulted	n.r.
[71]	Azo dyes	Descriptors selected by ant colony optimization	MLR	n.r. in the record consulted	n.r.
[72]	Anthraquinone dyes	Descriptors selected by ant colony optimization	MLR	n.r. in the record consulted	n.r.
[73]	Broad dye space	Learned structural representation	Deep neural network	n.r. in the record consulted	n.r.
[76]	Several dye classes (endpoint: molar absorption coefficient)	Molecular descriptors	Several machine-learning models	n.r. in the record consulted	n.r.
[7]	Azo photoswitches (798)	CircuS and ChyLine fragment counts	Support vector machine	Cross-validated RMSE 21.6 nm	R^2 = 0.905
[18]	Azo dyes (197; 160 training / 37 test)	TD-DFT descriptors, B3LYP/6-31G(d,p), SMD	Gaussian process regression	LOO R^2 = 0.837, RMSE 18.9 nm; 10-fold R^2 = 0.832, RMSE 21.7 nm	R^2 = 0.736, RMSE 31.5 nm

n.r. = not reported in the record consulted; several of the earlier studies are indexed without an accessible abstract, so their model statistics could not be verified and are deliberately left blank rather than estimated.

7. TOWARDS AN INTEGRATED, GREENER DEVELOPMENT WORKFLOW

The pieces described above can be assembled into the workflow of Figure 04, which is neither exotic nor expensive. A candidate coupler set is defined; each candidate is optimized in its analytically relevant protonation state with an implicit solvent model; global indices are computed to check that the coupler is nucleophilic enough to pair with the diazonium ion derived from the specific drug; condensed Fukui functions identify the expected coupling position; TD-DFT provides a first estimate of λ_{max} for the predicted product, with both tautomers computed where a hydroxy-azo product is expected; and a QSPR model, if one exists inside whose applicability domain the candidates fall, ranks them. Only the top two or three candidates then go to the bench. On a reasonable estimate this cuts reagent consumption during optimization by roughly an order of magnitude, which is a green analytical chemistry argument as much as an economic one [84].

That saving should be documented rather than asserted, and the metrics for doing so are mature. The Analytical Eco-Scale offers a simple penalty-point score [85], GAPI and its complementary extension grade every stage of a procedure including reagent preparation [86, 87], and AGREE converts the twelve principles into a single value with an interpretable pictogram [88]. Because greenness alone can be achieved by making a method useless, practicality and analytical performance need to be scored alongside it, which is the purpose of BAGI [89] and of the RGB and White Analytical Chemistry frameworks [90, 91]. A recent oxytetracycline assay that combined diazotization-coupling chemistry with a flatbed-scanner microplate readout and an explicit greenness evaluation shows how naturally these strands come together [92].

Two further developments make the case stronger. Miniaturization into microwell plates cuts reagent volumes to a fraction of the batch procedure while raising throughput [93], and flow-injection formats do something similar in a continuous mode [94],[54]. Smartphone digital image colorimetry removes the spectrophotometer altogether for field

screening [95]. All three amplify the value of getting the reagent right computationally beforehand, because in a miniaturized or instrument-free format there is much less room to compensate for a poorly chosen chromogen by simply using more of it. Finally, whatever route is taken, the assay itself must be validated to the current regulatory expectation. ICH Q2 (R2) sets out the validation characteristics [96], adopted as final guidance in the United States in 2024 [97], while Q14 introduces the analytical target profile and a risk-based development logic that fits a computationally guided reagent selection rather well [98].

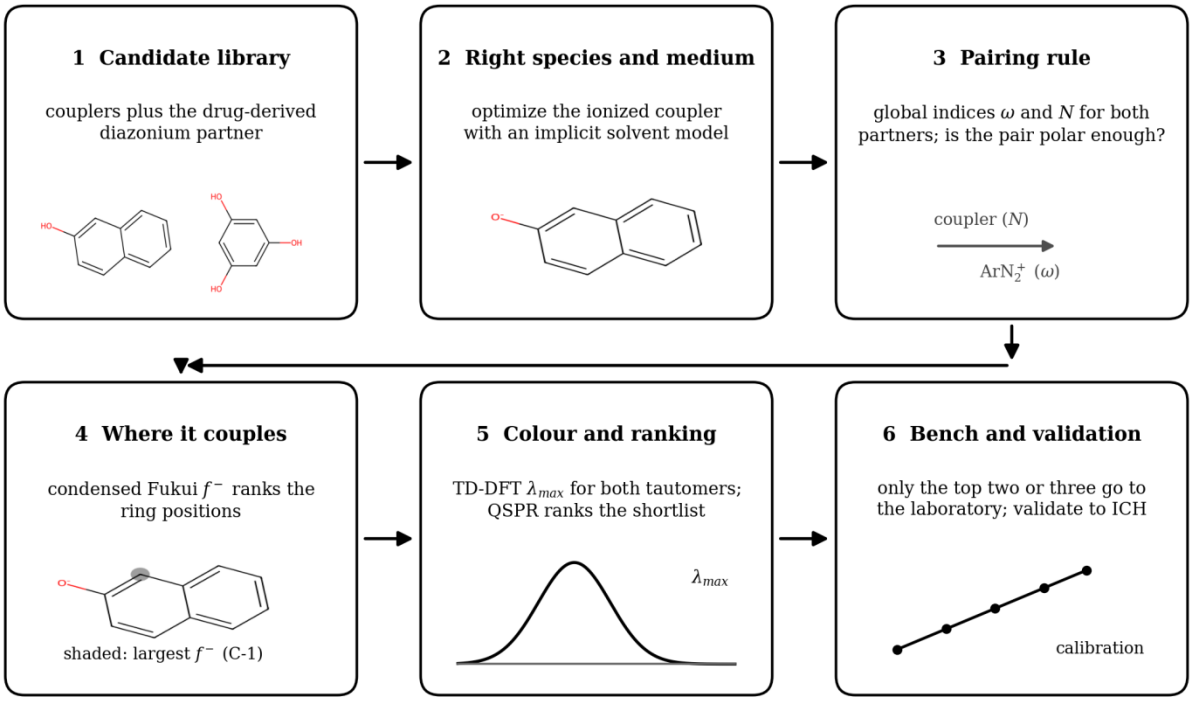

Figure 04: Proposed DFT- and QSPR-guided workflow for coupling-reagent selection, from candidate library through descriptor computation and virtual ranking to bench verification and validation.

8. GAPS, LIMITATIONS AND WHAT SHOULD BE REPORTED

The honest summary is that the computational literature and the analytical literature on azo chromogens have developed in near-isolation. Papers that calculate carefully tend to be about dyeing or photoswitching, and papers that measure carefully tend to treat computation as decoration. Bridging that gap requires, first, that calculations be done on the right species, meaning the ionized coupler and the actual product tautomer in the actual medium, and second, that predictions be reported before rather than after the experiment.

Several specific shortcomings recur often enough to be worth naming. Descriptors are frequently computed in the gas phase for reactions run in buffered water. Only one tautomer is modelled. The diazonium partner is often omitted entirely, so an electrophilicity-nucleophilicity pairing cannot be assessed. Molar absorptivity, the quantity most closely tied to the detection limit, is almost never predicted, only measured and reported afterwards. And where a QSPR model is invoked, the applicability domain is rarely stated, which makes the prediction unverifiable in principle.

Table 5 gathers this into a checklist. A modest set of reporting requirements would address most of this: the protonation state and tautomer used, the functional, basis set and solvation model, the computed global indices for both partners, the condensed Fukui indices at the candidate coupling sites, the predicted and observed λ_{max} with the deviation stated explicitly, and for QSPR the training set size, the external validation statistics and the applicability-domain check. None of this is burdensome, and it would make computational claims comparable across laboratories, which at present they are not.

Table 05: Proposed minimum computational and experimental reporting set for studies claiming DFT or QSPR support for the selection of an azo coupling reagent.

Item	What should be stated	Why it matters
Protonation state	Whether the neutral coupler or its anion was calculated	The anion is the species that reacts; the neutral form gives misleading descriptors
Tautomer	Which tautomer of a hydroxy-azo product was modelled, and whether both were computed	The two tautomers differ in colour; comparing one to a mixed experimental spectrum is not a valid test

Item	What should be stated	Why it matters
Level of theory	Functional, basis set and solvation model	Deviations of TD-DFT λmax depend strongly on all three
Both partners	Descriptors for the coupler and for the drug- derived diazonium ion	A pairing rule needs two numbers, not one
Local descriptors	Condensed Fukui indices at the candidate coupling positions	Establishes the predicted regiochemistry before synthesis
Predicted vs observed	λmax from calculation and from measurement, with the deviation in nm	Turns the calculation into a testable claim
Molar absorptivity	Calculated oscillator strength alongside the measured ε	ε, not λmax, sets the detection limit
QSPR training set	Number of compounds, chemical classes and the data source	Defines what the model has actually seen
QSPR validation	External test-set statistics and y-randomization	Internal cross-validation alone is not evidence of predictivity
Applicability domain	The domain definition used and whether the candidates fall inside it	Outside the domain, a confident prediction is meaningless
Colour stability	Stability window with the temperature at which it was measured	Azo degradation rates rise steeply with temperature
Greenness and practicality	AGREE / GAPI / Eco-Scale plus BAGI or an RGB-12 score	Lets the saving from virtual screening be documented rather than asserted

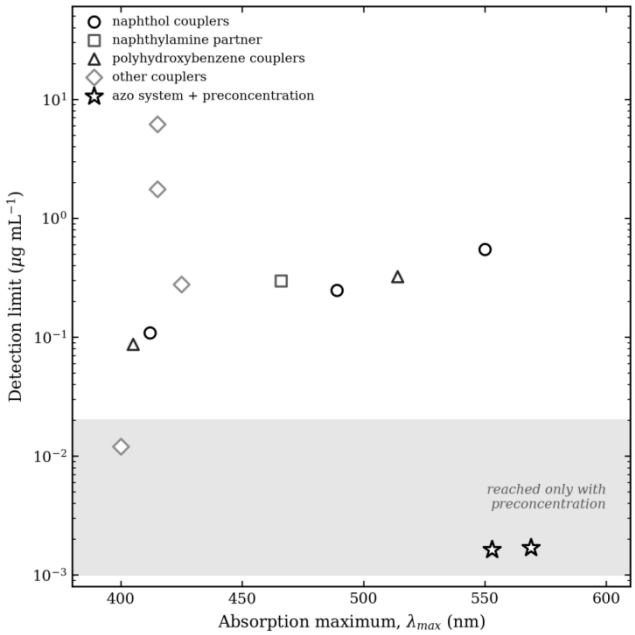

Figure 05: Reported absorption maximum plotted against detection limit for the azo systems compiled in Table 2, with markers coded by coupler family; the shaded band marks the sensitivity range reached only when the coloured product is preconcentrated.

9. CONCLUSION

Azo coupling has been used analytically for well over a century, and it works. What has been missing is a principled account of why one coupler outperforms another, and the tools to make that judgement before reagents are consumed. The evidence assembled here suggests that such an account is within reach. The reactive species is the ionized coupler; its nucleophilicity and the electrophilicity of the drug-derived diazonium ion together set the rate and the working pH; condensed Fukui functions locate the coupling site; and TD-DFT reproduces the absorption maximum of the product to within roughly 6-12 nm when the calculation is set up honestly. QSPR and machine learning extend this from single molecules to libraries, with external performance now approaching

an R^2 of 0.9 for λ_{max}, though molar absorptivity and colour stability remain essentially unmodelled and are arguably the more important endpoints for an analyst. Progress from here depends less on better theory than on better practice: calculating the species that actually reacts, reporting predictions before measurement, and stating applicability domains. If those habits take hold, coupling-reagent selection can stop being an empirical screen and become a design exercise.

10. FUNDING
The author declares that no funds, grants, or other financial support were received for the preparation of this manuscript. The work was carried out using the ordinary academic and computational resources of the Department of Chemistry, College of Education, University of Al-Qadisiyah, Al-Diwaniyah, Iraq.

11. ACKNOWLEDGEMENT
The author is grateful to the Department of Chemistry, College of Education, University of Al-Qadisiyah, Al-Diwaniyah, Iraq, for providing the library access and computing facilities used during the preparation of this review.

12. CONFLICT OF INTEREST
The author declares that he has no known competing financial interests, personal relationships, or other conflicts of interest that could have appeared to influence the work reported in this manuscript.

13. INFORMED CONSENT
Not applicable. This article is a review of the previously published literature and did not involve any human participants, human data, human tissue, or identifiable personal information; therefore, no informed consent was required.

14. ETHICAL STATEMENT
Not applicable in respect of experimental ethics: this article does not report any study involving human participants or animals performed by the author. All the material discussed is taken from previously published sources, which are properly cited and acknowledged. The author further confirms that the manuscript is original, has not been published elsewhere in whole or in part, is not under consideration by any other journal, and has been prepared in accordance with accepted standards of publication ethics, including the avoidance of plagiarism, data fabrication, and improper attribution.

15. AUTHOR CONTRIBUTION
Layth Samir Jasim Al-Hayder is the sole author of this manuscript. He was solely responsible for the conceptualization and design of the review, the literature search and data curation, the computational work, the preparation of all tables and figures, and the writing of the original draft as well as its subsequent review and editing. The author has read and approved the final version of the manuscript submitted for publication.

16. REFERENCES
1. Zollinger H. The kinetics of the diazo coupling reaction. Chemical Reviews, 1952, 51(2), 347-361. https://doi.org/10.1021/cr60159a004
2. Wistar R., Bartlett P.D. Kinetics and mechanism of the coupling of diazonium salts with aromatic amines in buffer solutions. Journal of the American Chemical Society, 1941, 63(2), 413-417. https://doi.org/10.1021/ja01847a019
3. Parr R.G., von Szentpály L., Liu S. Electrophilicity index. Journal of the American Chemical Society, 1999, 121(9), 1922-1924. https://doi.org/10.1021/ja983494x
4. Domingo L.R., Pérez P. The nucleophilicity N index in organic chemistry. Organic and Biomolecular Chemistry, 2011, 9(20), 7168-7175. https://doi.org/10.1039/c1ob05856h
5. Jacquemin D., Perpète E.A., Ciofini I., Adamo C. On the TD-DFT UV/vis spectra accuracy: the azoalkanes. Theoretical Chemistry Accounts, 2008, 120(4), 405-410. https://doi.org/10.1007/s00214-008-0424-9
6. El-Rahman M.A., Alsubaie M.S., El-Atawy M.A., Alharbi H.Y., Aljohani M.S., Alrashdi S., Omar A.Z., Hamed E.A., et al. Synthesis, DFT analysis, and dyeing performance of 4,4′-dihydroxy-3-substituted azobenzene disperse dyes with comparative evaluation of aqueous and DMF-based application systems. Journal of Fluorescence, 2026, 36(5), 3283-3298. https://doi.org/10.1007/s10895-026-04754-z
7. Byadi S., Hashim P.K., Sidorov P. Predictive modeling of visible-light azo-photoswitches' properties using structural features. Journal of Cheminformatics, 2025, 17(1), 42. https://doi.org/10.1186/s13321-025-00993-7
8. Tshilumba P.M., Ilangala A.B., Mbinze Kindenge J., Kasongo I.M., Kikunda G., Rongorongo E., Impele A.B., Marini Djang'eing'a R., et al. Detection of substandard and falsified antibiotics sold in the Democratic Republic of the Congo using validated HPLC and UV-visible spectrophotometric methods. American Journal of Tropical Medicine and Hygiene, 2023, 109(2), 480-488. https://doi.org/10.4269/ajtmh.23-0045
9. Vashistha V.K., Bala R., Pullabhotla R.V.S.R. Derivatizing agents for spectrophotometric and spectrofluorimetric determination of pharmaceuticals: a review. Journal of Taibah University for Science, 2023, 17(1), 2206363. https://doi.org/10.1080/16583655.2023.2206363
10. Abdul Galil M.S., Abdulalem F.R., Abdulqawi N., Mohammed S.O., Al-qubati M., Abdallah H.M.

Advancements in azo-based spectrophotometric techniques for pharmaceutical and environmental analysis via diazotization-coupling reactions. Discover Chemistry, 2026, 3(1), 107. https://doi.org/10.1007/s44371-026-00513-y

11. Alnemari R.M., Alaqel S.I., Almalki A.H., Abduljabbar M.H., Alqahtani A.S., Abdelazim A.H. Adopted green spectrophotometric determination of futibatinib based on diazo coupling with 1-naphthol and assisted computational calculations. Journal of Photochemistry and Photobiology A: Chemistry, 2025, 466, 116396. https://doi.org/10.1016/j.jphotochem.2025.116396
12. Dixit R.B., Patel J.A. Spectrophotometric determination of paracetamol drug using 8-hydroxyquinoline. International Journal of Pharmaceutical Sciences and Research, 2014, 5(6), 2393-2397. https://doi.org/10.13040/IJPSR.0975-8232.5(6).2393-97
13. Sultan S.H., Majed Z.W. Spectrophotometric determination of bromhexine hydrochloride by diazotization and coupling method in its pharmaceutical preparations. Iraqi Journal of Science, 2020, 61(9), 2172-2181. https://doi.org/10.24996/ijs.2020.61.9.3
14. Abdulhadi R.Z., Mohammed D.H. Spectrophotometric method for determination of cefixime in its pure form and in pharmaceutical preparations using diazotization reaction and coupling with chromotropic acid reagent. International Journal of Health Sciences, 2022, 6(S4), 12483-12495. https://doi.org/10.53730/ijhs.v6nS4.12052
15. Gałuszka A., Migaszewski Z., Namieśnik J. The 12 principles of green analytical chemistry and the SIGNIFICANCE mnemonic of green analytical practices. TrAC Trends in Analytical Chemistry, 2013, 50, 78-84. https://doi.org/10.1016/j.trac.2013.04.010
16. Pankratov A.N. Analytical azo coupling reactions: a quantum-chemical consideration. Journal of Analytical Chemistry, 2005, 60(10), 920-929. https://doi.org/10.1007/s10809-005-0210-y
17. Geerlings P., De Proft F., Langenaeker W. Conceptual density functional theory. Chemical Reviews, 2003, 103(5), 1793-1874. https://doi.org/10.1021/cr990029p
18. Fang Y., Cao C., Yin D., Luo G., Cheng Y., Wang Q. Interpretable machine learning integrated with TD-DFT descriptors and SHAP analysis for predicting the maximum absorption wavelength of azo dyes. RSC Advances, 2025, 15(58), 50065-50075. https://doi.org/10.1039/D5RA07578E
19. Zollinger H. Reactivity and stability of arenediazonium ions. Accounts of Chemical Research, 1973, 6(10), 335-341. https://doi.org/10.1021/ar50070a002
20. Gabsi W., Boubaker T., Goumont R. Azo-coupling reactions of para-X-benzenediazonium cations with 3-ethoxythiophene in acetonitrile. International Journal of Chemical Kinetics, 2016, 48(5), 266-273. https://doi.org/10.1002/kin.20989
21. El Abed R., Slama T., Mahdhaoui F., Boubaker T. C-N coupling of 3-aminothiophene with substituted benzenediazonium cations: carbon nucleophilicity, hyper-ortho effects, and predictive modeling of structural analogs. ChemPhysChem, 2025, 26(24), e202500553. https://doi.org/10.1002/cphc.202500553
22. Ismail V.S., Mohammed S.A., Juju S.T., Abdullah K.M., Ibrahim D.H., Mala R.K., Fathulla H.F., Sharif S.M. Spectrophotometric determination of paracetamol in pharmaceuticals by diazotization and coupling reaction with resorcinol and 1-naphthol. Science Journal of University of Zakho, 2026, 14(2), 351-357. https://doi.org/10.25271/sjuoz.2026.14.2.1620
23. Abd Alkareem E., Farhan Abd Al-karim N., Mahmoud I.I. Synthesis of new azo compounds and their application for a simple spectrophotometric determination of methyldopa drug using anthranilic acid and 2-aminopyrimidine as reagents. Journal of the Turkish Chemical Society Section A: Chemistry, 2023, 10(3), 621-632. https://doi.org/10.18596/jotcsa.1234028
24. Al-Uzri W.A. Determination of phenylephrine hydrochloride in pharmaceutical preparations using spectrophotometric method. Asian Journal of Pharmaceutical and Clinical Research, 2019, 12(5), 339-343. https://doi.org/10.22159/ajpcr.2019.v12i5.32339
25. Băldea I., Ghirișan A., Panea I. Kinetic studies of the azo coupling reaction between 1-(4-hydroxy-6-methylpyrimidin-2-yl)-3-methylpyrazolin-5-one and substituted benzenediazonium salts. Journal of the Chemical Society, Perkin Transactions 2, 1992, (10), 1715-1719. https://doi.org/10.1039/P29920001715
26. Skrabal P., Zollinger H. Mechanism of azo coupling reactions. Part XXXV. pH-dependence and ortho/para ratio in coupling reactions of aminohydroxynaphthalenesulfonic acids. Dyes and Pigments, 1988, 9(3), 201-207. https://doi.org/10.1016/0143-7208(88)85009-5
27. Kaminski R., Lauk U., Skrabal P., Zollinger H. Mechanism of azo coupling reactions XXXIII. pH-dependence and micromixing effects on the product distribution of couplings with 6-amino-4-hydroxy-2-naphthalenesulfonic acid. Helvetica Chimica Acta, 1983, 66(7), 2002-2017. https://doi.org/10.1002/hlca.19830660712

28. Challis B.C., Rzepa H.S. The mechanism of diazo-coupling to indoles and the effect of steric hindrance on the rate-limiting step. Journal of the Chemical Society, Perkin Transactions 2, 1975, (11), 1209-1217. https://doi.org/10.1039/P29750001209
29. Kelly R.P., Penton J.R., Zollinger H. Mechanisms of diazo coupling reactions. Part XXXII. The diazoamino rearrangement in 20% acetonitrile/aqueous buffers. Helvetica Chimica Acta, 1982, 65(1), 122-132. https://doi.org/10.1002/hlca.198206501 12
30. Schotten C., Leprevost S.K., Yong L.M., Hughes C.E., Harris K.D.M., Browne D.L. Comparison of the thermal stabilities of diazonium salts and their corresponding triazenes. Organic Process Research and Development, 2020, 24(10), 2336-2341. https://doi.org/10.1021/acs.oprd.0c00162
31. Diener H., Zollinger H. Mechanism of azo coupling reactions. Part 34. Reactivity of five-membered ring heteroaromatic diazonium ions. Canadian Journal of Chemistry, 1986, 64(6), 1102-1107. https://doi.org/10.1139/v86-185
32. Iwamoto H., Kobayashi H., Murer P., Sonoda T., Zollinger H. Mechanism of azo coupling reactions. Part XXXVI. The relationship between the structure and the catalytic activity of anionic phase-transfer catalysts in azo coupling reactions. Bulletin of the Chemical Society of Japan, 1993, 66(9), 2590-2602. https://doi.org/10.1246/bcsj.66.2590
33. Zollinger H. Diazo Chemistry I: Aromatic and Heteroaromatic Compounds. VCH, Weinheim, 1994, 453 pp. ISBN 3-527-29213-6.
34. Zollinger H. Color Chemistry: Syntheses, Properties and Applications of Organic Dyes and Pigments, 3rd revised edition. Verlag Helvetica Chimica Acta, Zurich / Wiley-VCH, Weinheim, 2003, 637 pp. ISBN 3-906390-23-3.
35. Balam-Villarreal J.A., López-Mayorga B.J., Gallardo-Rosas D., Toscano R.A., Carreón-Castro M.P., Basiuk V.A., Cortés-Guzmán F., López-Cortés J.G., et al. π-Extended push–pull azo-pyrrole photoswitches: synthesis, solvatochromism and optical band gaps. Organic and Biomolecular Chemistry, 2020, 18(8), 1657-1670. https://doi.org/10.1039/c9ob02410g
36. Sinan R. Spectrophotometric determination of metoclopramide hydrochloride in pharmaceutical tablets, by diazotization-coupling method with 1-naphthol as the coupling agent. Baghdad Science Journal, 2010, 7(1), 704-712. https://doi.org/10.21123/bsj.2010.7.1.704-712
37. Ahmad N.M., Mohammed I.S. Azo coupling reaction for spectrophotometric determination of sulfanilamide using β-naphthol as a reagent. Iraqi Journal for Applied Science, 2024, 1(2), 46-55. https://doi.org/10.69923/x09a3a81
38. Alani M., Al Samarrai E.T., Majeed S.R. Development of a spectrophotometric method to determination minoxidil by diazotization-coupling reaction with sulfanilic acid. Samarra Journal of Pure and Applied Science, 2025, 7(2), 31-44. https://doi.org/10.54153/sjpas.2025.v7i2.954
39. Darweesh S.A. Spectrophotometric determination of cefixime following simple diazotization and coupling with β-naphthol. Iraqi Journal of Pharmaceutical Sciences, 2017, 26(2), 1-6. https://doi.org/10.31351/vol26iss2pp1-6
40. Genç F., Milcheva N.P., Hristov D.G., Gavazov K.B. A simple cloud point extraction-spectrophotometric method for total vanadium determination using 4-(2-thiazolylazo)resorcinol and H2O2. Chemical Papers, 2020, 74(6), 1891-1901. https://doi.org/10.1007/s11696-019-01038-8
41. Gavazov K.B., Racheva P.V., Milcheva N.P., Divarova V.V., Kiradzhiyska D.D., Genç F., Saravanska A.D. Use of a hydrophobic azo dye for the centrifuge-less cloud point extraction-spectrophotometric determination of cobalt. Molecules, 2022, 27(15), 4725. https://doi.org/10.3390/molecules27154725
42. Fattahi Bafghi M.R., Haji Shabani A.M., Dadfarnia S., Nozohour Yazdi M. Dispersive liquid-liquid microextraction followed by magnetic nanoparticles retrieval of extract for separation and preconcentration of tetracycline from real samples before its selective spectrophotometric determination based on azo dye formation. Separation Science Plus, 2022, 5(8), 407-415. https://doi.org/10.1002/sscp.202200018
43. Özen A.S., Doruker P., Aviyente V. Effect of cooperative hydrogen bonding in azo-hydrazone tautomerism of azo dyes. The Journal of Physical Chemistry A, 2007, 111(51), 13506-13514. https://doi.org/10.1021/jp0755645
44. Adegoke O.A. Relative predominance of azo and hydrazone tautomers of 4-carboxyl-2,6-dinitrophenylazohydroxynaphthalenes in binary solvent mixtures. Spectrochimica Acta Part A: Molecular and Biomolecular Spectroscopy, 2011, 83(1), 504-510. https://doi.org/10.1016/j.saa.2011.08.075
45. Adegoke O.A., Idowu S.O. Solvatochromic behaviours and structure-spectra relationships of 4-carboxyl-2,6-dinitrophenylazohydroxynaphthalenes. Spectrochimica Acta Part A: Molecular and Biomolecular Spectroscopy, 2010, 75(2), 719-727. https://doi.org/10.1016/j.saa.2009.11.045
46. Taheri B., Zakerhamidi M.S., Shamkhali A.N., Kian R., Sadeghan A.A. Solvent polarity effect on

photophysical properties of some aromatic azo dyes with focus on tautomeric and toxicity competition. Scientific Reports, 2025, 15(1), 15716. https://doi.org/10.1038/s41598-025-00001-w

47. Dostanić J., Mijin D., Uščumlić G., Jovanović D.M., Zlatar M., Lončarević D. Spectroscopic and quantum chemical investigations of substituent effects on the azo-hydrazone tautomerism and acid-base properties of arylazo pyridone dyes. Spectrochimica Acta Part A: Molecular and Biomolecular Spectroscopy, 2014, 123, 37-45. https://doi.org/10.1016/j.saa.2013.12.064
48. Altalbawy F., Darwish E., Medhat M., El-Zaiat S., Saleh H. Synthesis, characterization, tautomeric structure and solvatochromic behavior of novel 4-(5-arylazo-2-hydroxystyryl)-1-methylpyridinium iodide as potential molecular photoprobe. Materials, 2016, 9(12), 1022. https://doi.org/10.3390/ma9121022
49. Shamsipur M., Maddah B., Hemmateenejad B., Rouhani S., Haghbeen K., Alizadeh K. Multiwavelength spectrophotometric determination of acidity constants of some azo dyes. Spectrochimica Acta Part A: Molecular and Biomolecular Spectroscopy, 2008, 70(1), 1-6. https://doi.org/10.1016/j.saa.2007.07.006
50. Pach A., Zaryczny A., Podborska A., Luty-Błocho M. The role of ascorbic acid in the process of azo dye degradation in aqueous solution. Molecules, 2024, 29(15), 3659. https://doi.org/10.3390/molecules29153659
51. Khalaf N., Othman N. Diazo-coupling reaction in spectrophotometric determination of doxycycline in pure and its dosage forms. Egyptian Journal of Chemistry, 2023, 66(6), 171-177. https://doi.org/10.21608/ejchem.2022.152883.6619
52. Mohamed Ben-Hander G., Adam R., Abualassad R., Zrik R., Aljealani E., Al-Abbasi A. Spectrophotometric evaluation of paracetamol in pharmaceutical preparations using diazotization coupling reaction with alanine and tyrosine amino acids. Bulletin of the Chemical Society of Ethiopia, 2026, 40(4), 723-734. https://doi.org/10.4314/bcse.v40i4.1
53. Adegoke O.A., Quadri M.O. Novel spectrophotometric determinations of some cephalosporins following azo dye formation with p-dimethylaminobenzaldehyde. Arabian Journal of Chemistry, 2016, 9(Suppl. 2), S1272-S1282. https://doi.org/10.1016/j.arabjc.2012.02.005
54. Mohammed F.F., Abed S.S. Two spectrophotometric methods based on diazotization coupling reaction for determination of genistein in pure and supplement. Iraqi Journal of Science, 2023, 64(4), 1581-1591. https://doi.org/10.24996/ijs.2023.64.4.1
55. Lemos V.A., Santos E.S., Santos M.S., Yamaki R.T. Thiazolylazo dyes and their application in analytical methods. Microchimica Acta, 2007, 158(3), 189-204. https://doi.org/10.1007/s00604-006-0704-9
56. Issa Y.M., El-Hawary W.F., Youssef A.F., Senosy A.R. Spectrophotometric determination of sildenafil citrate in pure form and in pharmaceutical formulation using some chromotropic acid azo dyes. Spectrochimica Acta Part A: Molecular and Biomolecular Spectroscopy, 2010, 75(4), 1297-1303. https://doi.org/10.1016/j.saa.2009.12.068
57. Renny J.S., Tomasevich L.L., Tallmadge E.H., Collum D.B. Method of continuous variations: applications of Job plots to the study of molecular associations in organometallic chemistry. Angewandte Chemie International Edition, 2013, 52(46), 11998-12013. https://doi.org/10.1002/anie.201304157
58. Domingo L.R., Ríos-Gutiérrez M., Pérez P. Applications of the conceptual density functional theory indices to organic chemistry reactivity. Molecules, 2016, 21(6), 748. https://doi.org/10.3390/molecules21060748
59. Fonseca S., Santos L., Pereira R., Modesto-Costa L., da Cunha A.R., Siqueira M.R.S., Carvalho F.A.O., Andrade-Filho T., et al. A DFT analysis of electronic, reactivity, and NLO responses of a reactive orange dye: the role of Hartree-Fock exchange corrections. Journal of Molecular Modeling, 2022, 28(4), 85. https://doi.org/10.1007/s00894-022-05035-9
60. Al-Gaber M.A.I., Abd El-Lateef H.M., Khalaf M.M., Shaaban S., Shawky M., Mohamed G.G., Abdou A., Gouda M., et al. Design, synthesis, spectroscopic inspection, DFT and molecular docking study of metal chelates incorporating azo dye ligand for biological evaluation. Materials, 2023, 16(3), 897. https://doi.org/10.3390/ma16030897
61. El-Ghamry H.A., Gaber M., Napolion M.S., Atta A., Mohamed T.M., El-Wakiel N.A. Synthesis, characterization and theoretical studies of nitroxoline azo dye metal complexes and their role in mitigation of rheumatoid arthritis. Scientific Reports, 2025, 15(1), 20213. https://doi.org/10.1038/s41598-025-06518-4
62. Parr R.G., Yang W. Density functional approach to the frontier-electron theory of chemical reactivity. Journal of the American Chemical Society, 1984, 106(14), 4049-4050. https://doi.org/10.1021/ja00326a036
63. Yang W., Mortier W.J. The use of global and local molecular parameters for the analysis of the gas-phase basicity of amines. Journal of the American

Chemical Society, 1986, 108(19), 5708-5711. https://doi.org/10.1021/ja00279a008
64. Osman O.I. DFT study of the structure, reactivity, natural bond orbital and hyperpolarizability of thiazole azo dyes. International Journal of Molecular Sciences, 2017, 18(2), 239. https://doi.org/10.3390/ijms18020239
65. Surendranaik Y., Venkatesh T., Naik E. Synthesis, characterization, solvatochromic, and electrochemical investigation of novel 4-methyl coumarin fused azo dyes as an NLO material and their biological studies. Structural Chemistry, 2025, 36(1), 171-190. https://doi.org/10.1007/s11224-024-02359-5
66. Krawczyk P. Time-dependent density functional theory calculations of the solvatochromism of some azo sulfonamide fluorochromes. Journal of Molecular Modeling, 2015, 21(5), 118. https://doi.org/10.1007/s00894-015-2651-z
67. El-Rahman M.A., Omar A.Z., Kandeel A.R., Hamed E.A., El-Atawy M.A., Keshk R.M. Synthesis, characterization, and polyester dyeing performance of azo barbituric and thiobarbituric acid disperse dyes. Scientific Reports, 2025, 15(1), 13410. https://doi.org/10.1038/s41598-025-96473-x
68. Rashid M.A.M., Hayati D., Kwak K., Hong J. Theoretical investigation of azobenzene-based photochromic dyes for dye-sensitized solar cells. Nanomaterials, 2020, 10(5), 914. https://doi.org/10.3390/nano10050914
69. Shinde S.S., Jadhav A.G., Sekar N. Benzophenone based photostable fluorescent monoazo disperse dyes: synthesis, AIE, viscosity, UPF and TD-DFT study. SN Applied Sciences, 2020, 2(12), 2136. https://doi.org/10.1007/s42452-020-03732-9
70. Xu X., Luan F., Liu H., Cheng J., Zhang X. Prediction of the maximum absorption wavelength of azobenzene dyes by QSPR tools. Spectrochimica Acta Part A: Molecular and Biomolecular Spectroscopy, 2011, 83(1), 353-361. https://doi.org/10.1016/j.saa.2011.08.046
71. Atabati M., Khandani F. Ant colony optimization as a descriptor selection in QSPR modeling for prediction of λmax of azo dyes. Chinese Chemical Letters, 2012, 23(10), 1209-1212. https://doi.org/10.1016/j.cclet.2012.07.006
72. Atabati M., Zarei K., Borhani A. Ant colony optimization as a descriptor selection in QSPR modeling: estimation of the λmax of anthraquinones-based dyes. Journal of Saudi Chemical Society, 2016, 20, S547-S551. https://doi.org/10.1016/j.jscs.2013.03.009
73. Shao J., Liu Y., Yan J., Yan Z.-Y., Wu Y., Ru Z., Liao J.-Y., Miao X., et al. Prediction of maximum absorption wavelength using deep neural networks. Journal of Chemical Information and Modeling, 2022, 62(6), 1368-1375. https://doi.org/10.1021/acs.jcim.1c01449
74. Yap C.W. PaDEL-descriptor: an open source software to calculate molecular descriptors and fingerprints. Journal of Computational Chemistry, 2011, 32(7), 1466-1474. https://doi.org/10.1002/jcc.21707
75. Moriwaki H., Tian Y.-S., Kawashita N., Takagi T. Mordred: a molecular descriptor calculator. Journal of Cheminformatics, 2018, 10(1), 4. https://doi.org/10.1186/s13321-018-0258-y
76. Ksenofontov A.A., Lukanov M.M., Bocharov P.S. Can machine learning methods accurately predict the molar absorption coefficient of different classes of dyes? Spectrochimica Acta Part A: Molecular and Biomolecular Spectroscopy, 2022, 279, 121442. https://doi.org/10.1016/j.saa.2022.121442
77. Buglak A.A., Chebotaev P.P., Filatov M.A. Applications of QSPR and machine learning in molecular photonics. Advanced Optical Materials, 2025, 13(33), e01713. https://doi.org/10.1002/adom.202501713
78. Kaliszan R. QSRR: quantitative structure-(chromatographic) retention relationships. Chemical Reviews, 2007, 107(7), 3212-3246. https://doi.org/10.1021/cr068412z
79. Gramatica P. Principles of QSAR models validation: internal and external. QSAR and Combinatorial Science, 2007, 26(5), 694-701. https://doi.org/10.1002/qsar.200610151
80. Tropsha A. Best practices for QSAR model development, validation, and exploitation. Molecular Informatics, 2010, 29(6-7), 476-488. https://doi.org/10.1002/minf.201000061
81. Roy K., Mitra I., Kar S., Ojha P.K., Das R.N., Kabir H. Comparative studies on some metrics for external validation of QSPR models. Journal of Chemical Information and Modeling, 2012, 52(2), 396-408. https://doi.org/10.1021/ci200520g
82. Sahigara F., Mansouri K., Ballabio D., Mauri A., Consonni V., Todeschini R. Comparison of different approaches to define the applicability domain of QSAR models. Molecules, 2012, 17(5), 4791-4810. https://doi.org/10.3390/molecules17054791
83. Gramatica P. Origin of the OECD principles for QSAR validation and their role in changing the QSAR paradigm worldwide: an historical overview. Journal of Chemometrics, 2025, 39(3), e70014. https://doi.org/10.1002/cem.70014
84. Keith L.H., Gron L.U., Young J.L. Green analytical methodologies. Chemical Reviews, 2007, 107(6), 2695-2708. https://doi.org/10.1021/cr068359e

85. Gałuszka A., Migaszewski Z.M., Konieczka P., Namieśnik J. Analytical Eco-Scale for assessing the greenness of analytical procedures. TrAC Trends in Analytical Chemistry, 2012, 37, 61-72. https://doi.org/10.1016/j.trac.2012.03.013
86. Płotka-Wasylka J. A new tool for the evaluation of the analytical procedure: Green Analytical Procedure Index. Talanta, 2018, 181, 204-209. https://doi.org/10.1016/j.talanta.2018.01.013
87. Płotka-Wasylka J., Wojnowski W. Complementary green analytical procedure index (ComplexGAPI) and software. Green Chemistry, 2021, 23(21), 8657-8665. https://doi.org/10.1039/d1gc02318g
88. Pena-Pereira F., Wojnowski W., Tobiszewski M. AGREE - analytical GREEnness metric approach and software. Analytical Chemistry, 2020, 92(14), 10076-10082. https://doi.org/10.1021/acs.analchem.0c01887
89. Manousi N., Wojnowski W., Płotka-Wasylka J., Samanidou V. Blue applicability grade index (BAGI) and software: a new tool for the evaluation of method practicality. Green Chemistry, 2023, 25(19), 7598-7604. https://doi.org/10.1039/D3GC02347H
90. Nowak P.M., Kościelniak P. What color is your method? Adaptation of the RGB additive color model to analytical method evaluation. Analytical Chemistry, 2019, 91(16), 10343-10352. https://doi.org/10.1021/acs.analchem.9b01872
91. Nowak P.M., Wietecha-Posłuszny R., Pawliszyn J. White Analytical Chemistry: an approach to reconcile the principles of Green Analytical Chemistry and functionality. TrAC Trends in Analytical Chemistry, 2021, 138, 116223. https://doi.org/10.1016/j.trac.2021.116223
92. Puttasa P., Ngernpimai S., Tippayawat P., Park M.H., Teerasong S. A scanner-based microplate platform for high-throughput oxytetracycline detection using diazotization-coupling chemistry with greenness evaluation. Green Analytical Chemistry, 2026, 17, 100351. https://doi.org/10.1016/j.greeac.2026.100351
93. Alzoman N.Z., Darwish I.A. Development of green and high throughput microplate reader-assisted universal microwell spectrophotometric assay for direct determination of tyrosine kinase inhibitors in their pharmaceutical formulations irrespective the diversity of their chemical structures. Molecules, 2023, 28(10), 4049. https://doi.org/10.3390/molecules28104049
94. Bevanda A.M., Talić S., Ivanković A. Flow injection analysis toward green analytical chemistry. In: Płotka-Wasylka J., Namieśnik J. (eds), Green Analytical Chemistry. Springer, Singapore, 2019, pp. 299-323. https://doi.org/10.1007/978-981-13-9105-7_10
95. Ali D.S., Hassan R.O., Othman H.O., Taha H.T., Khaneghah A.M., Smaoui S. Revolutionizing detection: smartphone-powered colorimetry for the drugs and food analysis. Microchemical Journal, 2024, 205, 111228. https://doi.org/10.1016/j.microc.2024.111228
96. International Council for Harmonisation of Technical Requirements for Pharmaceuticals for Human Use. ICH Harmonised Guideline Q2(R2): Validation of Analytical Procedures. Step 4 version, adopted 1 November 2023. https://database.ich.org/sites/default/files/ICH_Q2(R2)_Guideline_2023_1130.pdf
97. US Food and Drug Administration, Center for Drug Evaluation and Research. Q2(R2) Validation of Analytical Procedures: Guidance for Industry. Final guidance, March 2024. https://www.fda.gov/regulatory-information/search-fda-guidance-documents/q2r2-validation-analytical-procedures
98. International Council for Harmonisation of Technical Requirements for Pharmaceuticals for Human Use. ICH Harmonised Guideline Q14: Analytical Procedure Development. Step 4 version, adopted 1 November 2023. https://www.ema.europa.eu/en/documents/scientific-guideline/ich-q14-guideline-analytical-procedure-development-step-5-revision-1_en.pdf